Mathematical modelling of some glass problems

EINDHOVEN UNIVERSITY OF TECHNOLOGY
Department of Mathematics and Computing Science

RANA 98-27
December1998

Mathematical Modelling of some Glass problems

by

K. Laevsky and R.M.M. Mattheij

Reports on Applied and Numerical Analysis
Department of Mathematics and Computing Science
Eindhoven University of Technology
P.O. Box 513
5600 MB Eindhoven, The Netherlands
ISSN: 0926-4507

Mathematical Modelling of some Glass Problems

K.Laevsky, R.M.M. Mattheij
Department of Mathematics and Computer Science,
Eindhoven University of Technology,
PO Box 513, 500 MB The Netherlands

Abstract

In studying glass morphology one often uses models, which describe it it as a strongly viscous Newtonian fluid. In this paper we shall study two types of problems encountered in glass technology. One is dealing with so called sintering, as plays a role in e.g. producing high quality glasses and the other with producing packing glass by the so called pressing. We give a Stokes model for describing these processes and discuss various aspects of the evolution of both forming problems. The sintering problem is solved by a boundary element method, for which an interesting analytical tool is employed in order to avoid numerical instabilities. The pressing problem actually deals with the morphology of a bottle or jar. Here we focus on simulating the glass flow. We first show how to deal with the temperature separately, by a suitable dimension analysis. Then we consider the flow of the glass in a domain with partially free, partially moving boundary. We give a number of numerical examples to sustain our result.

1 Introduction

For many years glass technology has been a craft based on expertise and experimental knowledge, reasonably sufficient to keep the products and the production competitive. Over the last twenty years mathematical modelling of the various aspects of the production has become increasingly decisive, however. This is induced in part by fierce competition from other materials, notably polymers, which e.g.

have found their way in the food packing industry. For another part this is a consequence of environmental concerns. It is not so much the waste (glass is 100 % recyclable, a strong advantage to most competitors) as well as the energy consumption. One should realise that the melting process of sand to liquid glass makes up for the largest cost factor of the product. To give an idea of the relative importance of the present industry some figures: In the European Union about 25 Megaton of glass is being produced, which represents 30 billion ECU worth. The industry employs over 200,000 people. Two thirds of the glass production is meant for packing ("jars and bottles"). Float glass (as used for panes) makes up for one quarter. The rest is for special products like CRTs and fibres.

Production of glass forms goes more or less along the following lines: First grains and additives, like soda, are being heated in a tank. This can be a device several tens of metres long and a few metres high and wide (width being larger than height). Here gas burners or electric heaters provide for the heat necessary to warm up the material till some 1400 °C. At one end the liquid glass comes out and is e.g. led to a pressing or blowing machine, or it ends up on a bed of liquid tin, where it spreads out to become float glass (for pane, wind shields etc.). In the latter case the major problems are to have a smooth flow from the oven on the bed and to control the spreading and flattening. The pressing and blowing process is used in producing packing glass. To obtain a glass form often a two-stage process is being used: first a blob of hot glass is pressed into a mould to form a so called *parison*. Here it is cooled down (the mould is kept at 500 °C) such that a small skin of solid glass is formed. This parison is then blown into its final shape. Such a pressing/blowing machinery can produce a number of products at the same time; as a result a more or less steady flow of glass products is coming out on a belt, which then have to be cooled down further in a controlled way such that the remaining stresses are as small as possible (and thus the strength is optimal).

Sometimes only pressing is needed. This is the case in the production of CRTs. Here a stamp is pressed into liquid glass and after lifting it again a certain morphology should have been transferred onto the glass screen.

As a final application of glass we may mention fibres. Glass fibres are e.g. used to produce insulation material. A modern application is for transmitting optical signals. These optical fibres need to consist of very pure glass and have a low porosity. One of the processes to produce this is through a so called *sol-gel process* which amounts to chemical purification. The result of this are pure, though strong, glass particles. Through heating they melt together to a larger compact, a process which is called *sintering*. The eventual outcome of this is should be a dense glass compact [9].

All these processes involve the flow of the (viscous) glass in combination with heat exchange. Although these two are closely intertwined we shall show in this paper that they can often be decoupled, thus effectively leading to isothermal flow problems on one hand and temperature problems on the other. For some overviews, see e.g. [2] [14] [10] [13].

This paper is built up as follows. In Section 2 we shall derive the basic flow equations that will play a role in our models. Then Section 3 is devoted to the sintering problem. We shall explain how we can describe the sintering of two cylinders (circles) numerically. This is typical for a more general compact of glass particles, which, however, is too complicated to deal with. The subsequent section, Section 4, also gives an analytical method which can even handle the touching of two such cylinders. Then in Section 5 we discuss the second problem, the pressing of glass in a mould. We describe the model and pay special attention to the heat exchange problem. In Section 6 the evolutionary process of the glass flow is considered numerically. An important practical problem here is the numerical conservation of mass. This is discussed in Section 7.

2 Modeling

Glass may be viewed as a frozen liquid, i.e. it has an amorfic structure. At sufficiently high temperatures (say above 600 °C) it behaves like an incompressible Newtonian fluid, which means that for a given dynamic viscosity η, a velocity $\mathbf{v}$ and a pressure p, the stress tensor τ is given by

$$\tau = -p\mathbf{I} + \eta(\mathbf{grad}\,\mathbf{v} + \mathbf{grad}\,\mathbf{v}^T) \tag{2.1}$$

This constitutive relation should be used to close the equations that actually describe the motion of glass blob, the momentum equation (2.2) and the continuity equation (2.3):

$$\rho\left(\frac{\partial \mathbf{v}}{\partial t} + (\mathbf{grad}\,\mathbf{v})^T\mathbf{v}\right) = \rho\mathbf{f} + \mathbf{div}\,\tau, \tag{2.2}$$

where ρ denotes the mass density and $\mathbf{f}$ the volume forces on the blob,

$$\mathrm{div}\,\mathbf{v} = 0. \tag{2.3}$$

Using (2.1) in (2.2) we obtain

$$\rho\left(\frac{\partial \mathbf{v}}{\partial t} + (\mathbf{grad}\,\mathbf{v})^T\mathbf{v}\right) = \rho\mathbf{f} - \mathrm{grad}\,p + \mathbf{div}\left(\eta(\mathbf{grad}\,\mathbf{v} + \mathbf{grad}\,\mathbf{v}^T)\right) \tag{2.4}$$

In the two problems we shall study in this paper we anticipate the viscous forces ($\mathbf{div}\,\tau$) to dominate in (2.2). To see this we shall reformulate our equations in dimensionless form, for which we need some characteristic quantities.

First we remark that the only acting volume force in the process is gravity, so $\|\mathbf{f}\| \approx 10\, m/s^2$. We define

$$\tilde{\mathbf{f}} := \frac{1}{\|\mathbf{f}\|}\mathbf{f}. \tag{2.5}$$

The viscosity η is assumed to be constant, say $\eta_0 \approx 10^4\, kg/ms$. Normally there is no need to introduce a dimensionless viscosity, but we shall nevertheless do this. Thus, let since it may be highly temperature dependent

$$\tilde{\eta} := \frac{1}{\eta_0}\eta. \tag{2.6}$$

A typical average velocity V_0 (which is $10^{-1}\, m/s$ or much smaller), say $V_0 \approx 10^{-1}\, m/s$, can be used as a characteristic velocity. As a characteristic length scale we take $L(\approx 10^{-2}\, m$, or smaller). We now define the dimensionless quantities

$$\tilde{\mathbf{x}} := \frac{\mathbf{x}}{L}, \tag{2.7a}$$

$$\tilde{\mathbf{v}} := \frac{\mathbf{v}}{V_0}, \tag{2.7b}$$

$$\tilde{p} := \frac{L}{\eta_0 V_0}p. \tag{2.7c}$$

A proper choice as characteristic time scale is the ratio L/V_0 ($\approx 10^{-1}\, s$). So, let us finally define

$$\tilde{t} := \frac{V_0}{L}t. \tag{2.7d}$$

Substituting all dimensionless quantities into (2.3), (2.4) yields

$$Re\left(\frac{\partial \tilde{\mathbf{v}}}{\partial \tilde{t}} + (\mathbf{grad}\,\tilde{\mathbf{v}})^T\,\tilde{\mathbf{v}}\right) = \frac{Re}{Fr}\tilde{\mathbf{f}} - \operatorname{grad}\tilde{p} + \mathbf{div}\left(\tilde{\eta}\left(\mathbf{grad}\,\tilde{\mathbf{v}} + \mathbf{grad}\,\tilde{\mathbf{v}}^T\right)\right), \tag{2.8a}$$

$$\operatorname{div}\tilde{\mathbf{v}} = 0. \tag{2.8b}$$

All spatial derivatives in (2.8) have to be taken with respect to the dimensionless variable $\tilde{\mathbf{x}}$. In (2.8a) two dimensionless numbers appear, namely the *Reynolds number* (Re) and the quotient of the Reynolds number and the *Froude number* (Re/Fr),

defined by

$$Re := \frac{V_0 L \rho}{\eta_0}, \quad \frac{Re}{Fr} := \frac{\rho \|\mathbf{f}\| L^2}{\eta_0 V_0}.$$

The Reynolds number indicates the ratio between inertial forces and viscous forces and the quotient of the Reynolds number and the Froude number indicates the ratio between volume forces (i.e. gravity) and viscous forces. The two numbers are estimated by

$$Re \approx 10^{-4}, \quad \frac{Re}{Fr} \approx 10^{-3}. \tag{2.9}$$

From this we conclude that the viscous forces dominate indeed. Thus, the flow describing the equations are (rewritten in its dimensionless form)

$$\operatorname{grad} p = \mathbf{div}\left(\eta\left(\mathbf{grad}\,\mathbf{v} + \mathbf{grad}\,\mathbf{v}^T\right)\right), \tag{2.10a}$$

$$\operatorname{div} \mathbf{v} = 0. \tag{2.10b}$$

These equations of course the *Stokes creeping flow equations*. These Stokes equations require further boundary conditions in order to be able to solve the vector $\mathbf{v}$. Actually they will be kinematic constraints, changing with time t, describing the evolution of the blob. We shall specify these BC for the two situations in the subsequent section. They have in common that at least one part of the boundary is free. Hence, besides finding the velocity $\mathbf{v}(t)$ we then need to find this free boundary. The actual displacements $\mathbf{x}$ satisfy the ODE

$$\frac{d\mathbf{x}}{dt} = \mathbf{v}(\mathbf{x}). \tag{2.11}$$

Numerically we shall deal with these problems in a two stage sweep: Suppose we have a domain $\mathcal{G}(t)$, describing the glass blob. Then solve (2.10) (approximately) and use velocity field on the boundary to compute a new domain $\mathcal{G}(t + \Delta t)$, using (2.11) and the BC.

3 Viscous sintering

Sintering is the process of bringing a powder of metals, ionic crystals, or glasses (a compact) to such a high temperature that sufficient mobility is present to release the excess free energy of the surface of the powder , thereby joining the particles together. The driving force arises from the excess free energy of the surface of the

powder over that of the solid material. For a survey of the most important papers about sintering we refer to the book edited by Sōmiya and Moriyoshi [12].

We are interested in the case of sintering glasses, see also [11] [9]. There the material transport can be modelled as a viscous incompressible Newtonian volume flow, driven solely by surface tension (*viscous sintering*), i.e. the Stokes creeping flow equations hold. The geometry of such a sintering compact is usually very complex. Because of this it is impossible to give a deterministic description of the flow in such a compact as a whole. We shall therefore investigate simple geometries in 2-D only. For more general compacts see e.g. [15] [16] [8].

Let us denote the compact (blob) at time t by Ω_t and its boundary by Γ_t, see fig. 1 Then the driving force of the boundary movement is a tension in the direction of the normal $\mathbf{n}$; the latter being proportional to the local curvature, κ of the boundary. Thus we obtain

$$\tau\mathbf{n} = (\operatorname{div}\mathbf{n})\mathbf{n} = \kappa\mathbf{n}. \tag{3.1}$$

Our only interest is the movement of the boundary Γ, i.e. only the velocity at the boundary is required (from which we can calculate the shape evolution of the body directly). Therefore this problem is ideally suited to be solved numerically by a Boundary Element Method (BEM). To do this, we have to reformulate the problem as an integral equation over the boundary. This is done in terms of a boundary distribution of hydrodynamical single- and double-layer potentials, see also Ladyzhenskaya [7].

When the boundary is sufficiently "smooth", the integral formulation that can be derived for the Stokes equations at a point, say $\mathbf{x}$, reads in matrix notation (see also [6])

$$C\mathbf{v}(\mathbf{x}) + \int_\Gamma Q(\mathbf{x},\mathbf{y})\mathbf{v}d\Gamma_y = \int_\Gamma U(\mathbf{x},\mathbf{y})\mathbf{b}d\Gamma_y. \tag{3.2}$$

Here C, $Q(\mathbf{x},\mathbf{y})$ and $U(\mathbf{x},\mathbf{y})$ are 2×2 matrices with coefficients c_{ij}, q_{ij} and u_{ij}, $i, j = 1, 2$ respectively:

$$c_{ij} = \begin{cases} \delta_{ij} & \mathbf{x} \in \Omega \\ \frac{1}{2}\delta_{ij} & \mathbf{x} \in \Gamma, \end{cases} \tag{3.3}$$

$$q_{ij} = \frac{r_i r_j}{\pi(r_1^2 + r_2^2)^2} r_k n_k, \tag{3.4}$$

$$u_{ij} = \frac{1}{4\pi}\left[-\delta_{ij}\frac{1}{2}log[r_1^2 + r_2^2] + \frac{r_i r_j}{r_1^2 + r_2^2}\right], \tag{3.5}$$

where δ_{ij} is the Kronecker delta, $r_i := x_i - y_i$, $i, j = 1, 2$, and the vector $\mathbf{b}$ is the boundary curvature in the normal direction, i.e.

$$\mathbf{b} = \kappa \mathbf{n}. \tag{3.6}$$

The integral equation (3.2) (or, equivalently, the equations (1.3), (1.4) and (3.1)) which has to be solved for a fixed boundary, does not ensure a unique solution $\mathbf{v}$. Clearly, we need to add three extra conditions (equations) to account for the degrees of freedom with respect to translation and rotation.

We follow the approach of Hsiao, Kopp and Wendland [5], for making the integral equation (3.2) uniquely solvable for a fixed boundary. This is done by adding three additional variables w_i to this integral equation which prescribe the translation and rotation, i.e.

$$C\mathbf{v}(\mathbf{x}) + \int_\Gamma Q(\mathbf{x}, \mathbf{y})\mathbf{v}d\Gamma_y + V(\mathbf{x})\mathbf{w} = \int_\Gamma U(\mathbf{x}, \mathbf{y})\mathbf{b}d\Gamma_y, \tag{3.7}$$

where V is a 2×3 matrix defined by

$$V = \begin{bmatrix} 1 & 0 & x_2 \\ 0 & 1 & -x_1 \end{bmatrix}. \tag{3.8}$$

Now, three additional equations have to be given to ensure that the boundary velocity is defined uniquely. In order to prescribe the translation freedom, we formulate the problem to be stationary at a (reference) point in the fluid, say $\mathbf{x}^r$. With regard to this reference point the velocity of the boundary points is computed. The most natural choice for this reference point is the centre of mass: the point where the gravity forces would grip the body, thus:

$$\mathbf{v}(\mathbf{x}^r) = 0. \tag{3.9}$$

Using this, we derive from the integral formulation (3.2) and $\mathbf{x} = \mathbf{x}^r$ the following two equations

$$\int_\Gamma Q(\mathbf{x}^r, \mathbf{y})\mathbf{v}d\Gamma_y = \int_\Gamma U(\mathbf{x}^r, \mathbf{y})\mathbf{b}d\Gamma_y. \tag{3.10}$$

Furthermore we assume the tangential component of the velocity at the boundary to be zero, i.e.

$$\int_\Gamma (\mathbf{v}, \tau)d\Gamma = 0, \tag{3.11}$$

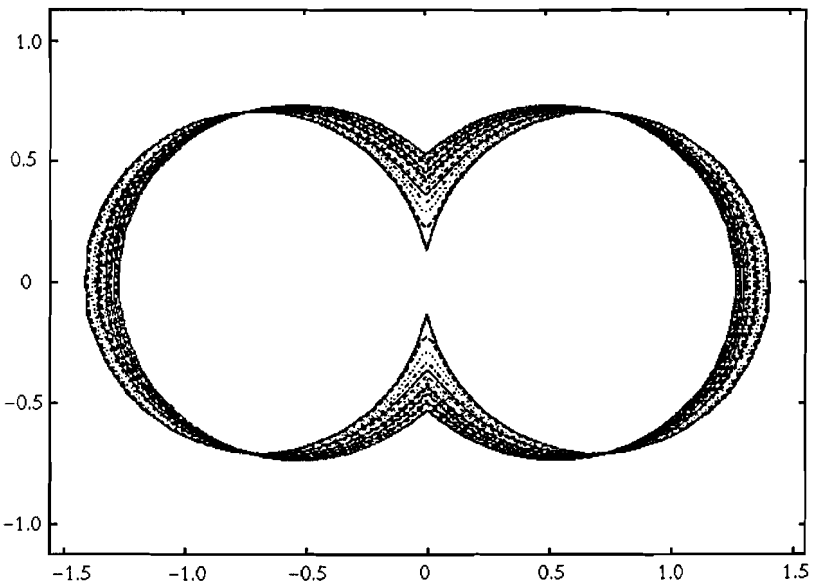

Figure 3.1: Two sintering cylinders with equal diameters. The same mesh is used through the simulation

where τ is the tangential vector of the boundary. Combining this with Stokes formula it follows from equation (3.11) that the flow in Ω is *irrotational.*

In a practical implementation we have to determine the grid on Γ in an appropriate way; for more see [16]. Special care has to be taken with respect to the computation of the curvature. Indeed, if we use finite differences to approximate differential quotients we are facing problems when the distance between gridpoints is too small. In fig.3.1 we have illustrated this for the coalescence of two circles (actually cylinders in a 3-D setting) the time after the actual touching took place. At this touching point a so called *neck* is developing at which the curvature is still extremely high. The results show numerical instability. In order to cure this problem we shall invoke some analytical tools first.

4 The Analytical Solution for the coalescence of two equal circles

In this section we give the analytical solution for the coalescence of two equal circles and we introduce some notation for the main properties of this solution. These are the initial radius R of both circles, the measure of contact between both circles and the boundary curvature at the contact.

The analytical solution for the evolution of two equal coalescing circles has been derived by Hopper [4]. He described the evolution of these circles in terms of a time-dependent mapping function $z = x + \mathbf{i}y = \Omega(\xi, t)$ of the unit circle, conformal on $|\xi| \leq 1$. The time evolution of the map was given in parametric form. In these papers, the equations derived are valid for the coalescence of two circles with initial radius $\frac{1}{2}\sqrt{2}$. Here it turns out that we may take

$$z = \frac{\sqrt{2}(1-\nu^2)e^{\frac{1}{2}\mathbf{i}\theta}}{1-\nu e^{2\mathbf{i}\theta}\sqrt{1+\nu^2}}, \tag{4.1}$$

where $e^{\mathbf{i}\theta}$ describes the contour of the unit circle and $\nu = \nu(t)$ is a function with values $\in [0, 1]$. For $\nu \to 1$ we have a touching of the two circles.

Following Hopper [3], we can derive parametric equations for the evolution of two coalescing circles both with initial radius R and centres $(R, 0)$ and $(-R, 0)$ each

$$\begin{aligned} x(\theta, \nu) &= \frac{(1-\nu^2)(1-\nu)R\sqrt{2}\cos\theta}{(1-2\nu\cos 2\theta+\nu^2)\sqrt{1+\nu^2}} \\ y(\theta, \nu) &= \frac{(1-\nu^2)(1+\nu)R\sqrt{2}\sin\theta}{(1-2\nu\cos 2\theta+\nu^2)\sqrt{1+\nu^2}} \end{aligned} \tag{4.2}$$

and for the time t (as function of ν)

$$t(\nu) = \frac{\pi R}{\sqrt{2}}\int_{\nu}^{1}\frac{dk}{k\sqrt{1+k^2}\mathrm{K}(k)}. \tag{4.3}$$

Here $\mathrm{K}(k)$ is the complete elliptic integral of the first kind defined by

$$\mathrm{K}(k) = \int_0^{\frac{\pi}{2}}\left(1-k^2\sin^2\phi\right)^{-\frac{1}{2}}d\phi. \tag{4.4}$$

The degree of coalescence is specified by the parameter ν, which decreases from 1 to 0 if time increases (t is going to infinity as $\nu \to 0$), and the boundary curve is specified by the parameter θ, which is varifying from 0 to 2π. Of course, at $t = 0$, both circles are making contact at the origin.

Of special interest is the region where the circles are touching. In our example, the line of contact is the y-axis during the evolution. Let r be the *contact radius* between both circles, and denote the point on the boundary at the line of contact in the positive direction by $\mathbf{x}^n$, i.e. $\mathbf{x}^n = (0, r)$. Recall that we called this point the *neck*.

In the analytical solution (4.2) the neck is occurring at $\theta = \pi/2$ during the evolution. Thus for the contact radius r, as a function of the parameter ν, the following holds

$$r(\nu) = y\left(\frac{\pi}{2}, \nu\right) = \frac{(1-\nu)R\sqrt{2}}{\sqrt{1+\nu^2}}. \tag{4.5}$$

Note that as $\nu \to 0$, i.e. $t \to \infty$, then $r \to R\sqrt{2}$, which is the radius of the circle the shape evolution is approaching as time increases.

By solving for the parameter ν as function of the contact radius r, we obtain from (4.5)

$$\nu = \nu(r) = \frac{2R^2 - r\sqrt{4R^2 - r^2}}{2R^2 - r^2}. \tag{4.6}$$

For the curvature of the neck, say κ_n, we can derive from the parametric equations (4.2)

$$\kappa_n(\nu) = \left.\frac{x_{\theta\theta}y_\theta - x_\theta y_{\theta\theta}}{(x_\theta^2 + y_\theta^2)^{\frac{3}{2}}}\right|_{\theta=\frac{\pi}{2}} = -\frac{(1 - 6\nu + \nu^2)\sqrt{1+\nu^2}}{(1-\nu)^3 R\sqrt{2}}. \tag{4.7}$$

Remark that as $\nu \to 0$, i.e. $t \to \infty$, then $\kappa_n \to -1/R\sqrt{2}$, as assumed. The derived neck curvature (4.7) can be written as a function of the contact radius r; from equations (4.6) and (4.7), we obtain

$$\kappa_n(r) = \frac{4R^2}{r^3} - \frac{3}{r}. \tag{4.8}$$

Using this formula, rather than a numerical derivation of the curvature gives satisfactory results, see fig.4.1.

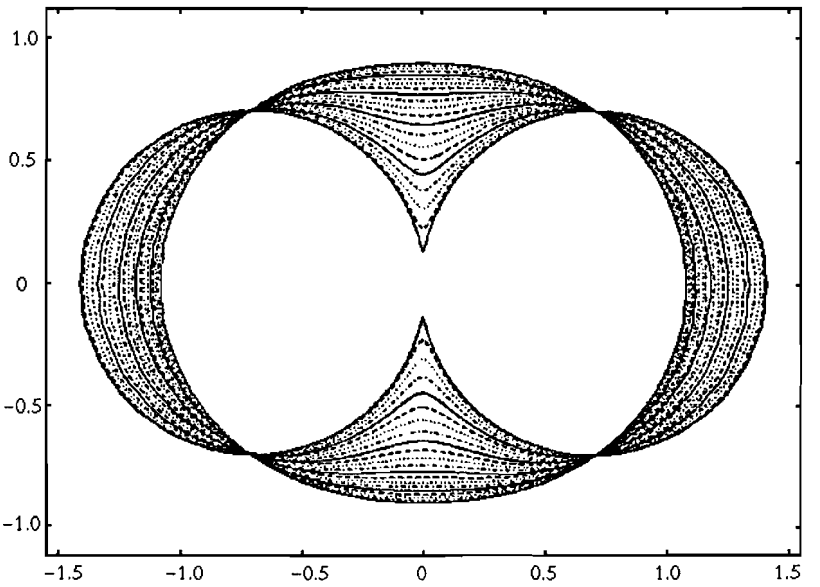

Figure 4.1: Two sintering cylinders with equal diameters. A mesh verification is done at each time step.

We can now also analyze the effect of a small perturbation of the initial contact radius r, $\Gamma + \varepsilon$, say, both circles having initial radius R (see fig.4.2). Although depicted in one graph they may represent the boundaries at different time points. So consider the parametric equations (4.2) as function of R and t (i.e. v). A measure for the difference between both shapes is given by the derivative of x, y with respect to R.

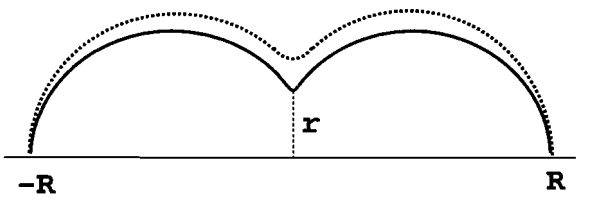

Figure 4.2: The coalescence of two equal circles.

Using (4.5), the parametric equations (4.2) can be written as

$$\begin{aligned} x(\theta, \nu) &= \frac{r(1-\nu^2)\cos\theta}{1+\nu^2-2\nu\cos 2\theta} \\ y(\theta, \nu) &= \frac{r(1+\nu^2)\sin\theta}{1+\nu^2-2\nu\cos 2\theta} \end{aligned} \tag{4.9}$$

We have to consider the equations (4.2) as a function of r (and t). The derivative of x and y with respect to r will then be a measure for the deviation between the two curves.

For the derivative of ν with respect to r, we obtain after squaring, taking the derivative of equation (4.5) and using the relation (4.6)

$$\frac{\partial \nu}{\partial r} = -\frac{2R^2(1-\nu)^2}{r^2\sqrt{4R^2-r^2}}. \tag{4.10}$$

Now define a normalized radius

$$\tilde{r} := r/(R\sqrt{2}),$$

then we derive the following relation between ν and $\tilde{r}$ (so r)

$$\frac{1-\nu}{1+\nu} = \frac{\tilde{r}}{\sqrt{2-\tilde{r}^2}}. \tag{4.11}$$

If we moreover write

$$\xi = \cos\theta,$$

we find, by taking the derivatives of (4.8) with respect to r, and restricting ourselves to the first quadrant, using (4.9),

$$\begin{aligned} \frac{\partial x}{\partial r} &= \frac{(1-\nu^2)\xi}{(1+\nu)^2-4\nu\xi^2} + \frac{2(1-\nu)^2[(1+\nu)^2-2(1+\nu^2)\xi^2]\xi}{\tilde{r}\sqrt{2-\tilde{r}^2}((1+\nu)^2-4\nu\xi^2)^2}, \\ \frac{\partial y}{\partial r} &= \frac{(1-\nu)^2\sqrt{1-\xi^2}}{(1+\nu)^2-4\nu\xi^2} - \frac{4(1+\nu)(1-\nu)^3\xi^2\sqrt{1-\xi^2}}{\tilde{r}\sqrt{2-\tilde{r}^2}((1+\nu)^2-4\nu\xi^2)^2}. \end{aligned} \tag{4.12}$$

Again our interest is mainly the neck region, i.e. ξ is small. Using (4.8) and (4.10)

we derive for (4.1)

$$\begin{aligned}\frac{\partial x}{\partial r} &= \frac{y\xi}{R\sqrt{2(1-\xi^2)(2-\tilde{r}^2)}} + \frac{y^2\xi\sqrt{2}[(1+\nu)^2 - 2(1+\nu^2)\xi^2]}{R(1-\xi^2)(1+\nu)^2(2-\tilde{r}^2)^{\frac{3}{2}}} \\ \frac{\partial y}{\partial r} &= \frac{y}{r} - \frac{2\sqrt{2}xy\xi}{rR(2-\tilde{r}^2)^{\frac{3}{2}}}.\end{aligned} \tag{4.13}$$

Using $0 \leq \tilde{r} < 1$, one may check that maximum absolute values in (4.13) are given by

$$\left|\frac{\partial x}{\partial r}\right| \leq \frac{y\xi}{R\sqrt{2(1-\xi^2)}}\left(1 + \frac{2y}{\sqrt{1-\xi^2}}\right), \quad \left|\frac{\partial y}{\partial r}\right| \leq \frac{y}{r}\left(1 + \frac{2\sqrt{2}x\xi}{R}\right). \tag{4.14}$$

In the neck region y is $O(r)$ and x small, i.e. from (4.14) we conclude that a small change of the contact radius r of the coalescing circles will not perturb the shape of the neck region, even when r is small.

The relation (4.8) for the (exact) neck curvature gives also information about the effect of a change of the contact radius r on this curvature. From (4.8) it follows that the derivative of the neck curvature, with respect to r, is given by

$$\frac{\partial \kappa_n}{\partial r} = -\frac{12R^2}{r^4} + \frac{3}{r^2}. \tag{4.15}$$

Thus a small change of the radius r has an $O\left(\frac{1}{r^4}\right)$ effect on the neck curvature, i.e. when the contact radius is small the curvature is changed dramatically. Conversely, we also have,

$$\frac{\partial r}{\partial \kappa_n} = -\frac{r^4}{12R^2 + 3r^2},$$

i.e. a change of the neck curvature gives only an $O(r^4)$ effect on the contact radius r.

A measure for the time difference between the shapes at time t and $\tilde{t}$ is given by the derivative of t with respect to r, i.e. taking the derivative of equation (4.3) and using (4.5), (4.9), we derive

$$\frac{\partial t}{\partial R} = \frac{\pi\sqrt{1+\nu^2}}{2\nu K(\nu)\sqrt{2-\tilde{r}^2}}. \tag{4.16}$$

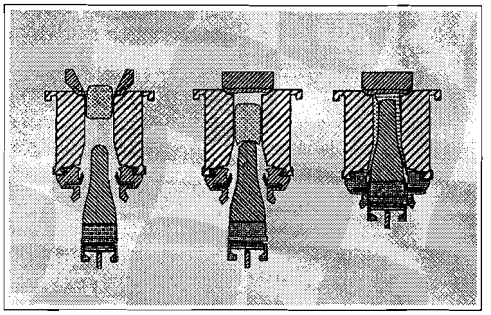

Figure 5.1: The pressing phase.

Using asymptotic expansions for $K(\nu)$ one can show that $\left|\frac{\partial t}{\partial R}\right|$ is small, when the time t is not too large. We conclude that the neck evolution is a smooth function of the time.

The above analysis shows that a small change of the contact radius is hardly perturbing the global shape of the neck region. Only the curvature of the neck (a local effect) is changed dramatically when r is small.

We finally remark that the curvature approximations here can be used more generally in the computation of rather complicated blobs. For more details see [16].

5 Pressing of glass

As stated in Section 1 there is a large variety of application of glass products. The previous sections dealt with particles of milimeter size. In this section we consider viscous flows arising in the production of packing glass, such as bottles and jars which are of order of $10\,cm$ size. Typically this is a two stage process. First a blob of glass is pressed in a *mould*, by a *plunger*, to a certain preform, the so called *parison* (see fig 5.1), which then is blown into the finally desired shape (see fig.5.2). We shall only consider the first stage, i.e. the pressing, here. Since the mould and the plunger are axisymmetric we shall assume the entire problem to be so. In practice the initial form of the glass blob may not be axisymmetric, but will not deviate too much from this form in a well controlled production process.

We thus can study an essential 2-D flow/energy problem in a time varyfying domain Ω_t as depicted in fig.5.3

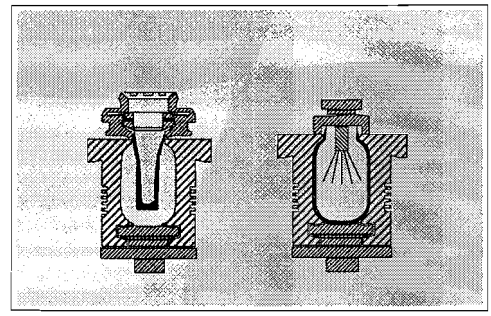

Figure 5.2: The blowing phase.

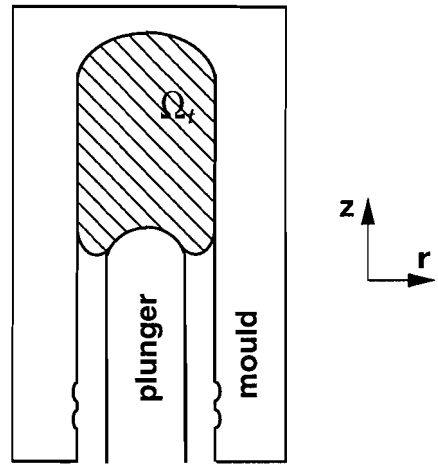

Figure 5.3: 2-D problem.

In cylindrical coordinates the Stokes equations (2.10) can be written as

$$\frac{\partial p}{\partial z} = \eta\left[\frac{\partial^2 u}{\partial z^2} + \frac{\partial^2 u}{\partial r^2} + \frac{1}{r}\frac{\partial u}{\partial r}\right],$$

$$\frac{\partial p}{\partial r} = \eta\left[\frac{\partial^2 v}{\partial z^2} + \frac{\partial^2 v}{\partial r^2} + \frac{1}{r}\frac{\partial v}{\partial r} - \frac{v}{r^2}\right], \tag{5.1 a}$$

$$0 = \frac{\partial u}{\partial z} + \frac{\partial v}{\partial z} + \frac{v}{r}. \tag{5.1 b}$$

Here u and v are the velocities in the z and the r directions respectively.

In contrast to the sintering problem we do not have an isothermal situation here, at least not in principle. As a consequence the viscosity η may not be constant, and in fact may vary quite wildly, as a function of the temperature. Note that the temperature T and the viscosity η of glass are related through the Vogel-Fulcher-Tamman relation [10]

$$\eta = K\exp(E_o/(T - T_0)). \tag{5.1}$$

Here K is some constant, E_0 the viscosity activation energy and T_0 a fixed temperature.

In dimensionless quantities (Section 2) the velocity and the temperature are coupled through the energy equation, written for the axisymmetric case for an incompressible stationary flow with constant heat conductivity and heat capacity as cf [1]

$$\left(v\frac{\partial T}{\partial r} + u\frac{\partial T}{\partial z}\right) = \frac{1}{Pe}\left(\frac{\partial^2 T}{\partial r^2} + \frac{1}{r}\frac{\partial T}{\partial r} + \frac{\partial^2 T}{\partial z^2}\right) + \tag{5.2}$$

$$\frac{Ec}{Re}\left(2\left(\frac{\partial u}{\partial z}\right)^2 + 2\left(\frac{\partial u}{\partial r}\right)\left(\frac{\partial v}{\partial z}\right) + 2\left(\frac{\partial v}{\partial r}\right)^2 + \left(\frac{\partial v}{\partial z}\right)^2 + \left(\frac{\partial u}{\partial r}\right)^2\right).$$

Here Ec is the *Eckhard* number, defined as (cf Section 2)

$$Ec := \frac{U^2}{c_p \Delta T}, \tag{5.3}$$

where c_p is the *specific heat* and ΔT the *temperature drop*. Pe is the *Peclet* number, defined as

$$Pe = \frac{\rho U L k}{\eta^2 c_p}, \tag{5.4}$$

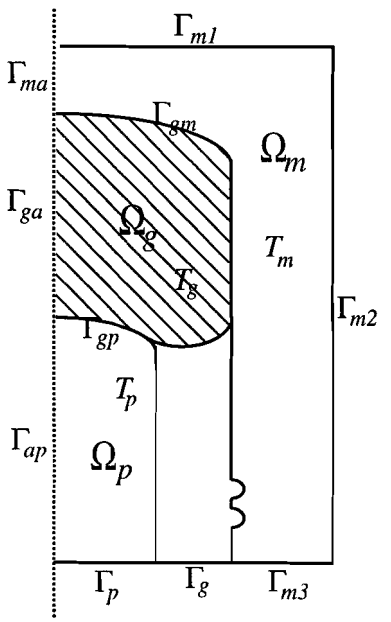

Figure 5.4: 2-D domain.

where k is the *thermal conductivity*. For glass we obtain

$$\frac{1}{Pe} := 6.2 \cdot 10^{-4}, \quad \frac{Ec}{Re} = 1.2 \cdot 10^{-4}.$$

Both are very small, so we can ignore the heat conduction and thermal production terms (the second and third term in equation (5.3)) and thus the energy equation simplifies to:

$$u\frac{\partial T}{\partial z} + v\frac{\partial T}{\partial r} = 0. \tag{5.5}$$

This equation is solved by the system

$$\frac{dz}{dt} = u, \quad \frac{dr}{dt} = v, \quad \frac{dT}{dt} = 0, \tag{5.6}$$

from which we see that the temperature remains constant along the streamlines. If we start with a uniform temperature field, it will remain uniform everywhere.

Now if we include the cooling of the wall we can do the following: Let Ω_p, Ω_g, Ω_m denote the plunger (p), glass (g) and mould (m) domains respectively (see

fig.5.4). Then the energy equation is simply given by

$$\frac{1}{k_i}\frac{\partial T_i}{\partial t} = \Delta T_i, \quad i \in \{p, g, m\}, \tag{5.7}$$

where k_i is the thermal conductivity. One can estimate the numerical values of these to find

$k_m = k_g = 6.2 \cdot 10^{-7}$ [m^2/s], thermal diffusivity.
$k_p = k_m = 1.7 \cdot 10^{-5}$[m^2/s], thermal diffusivity.

We observe that $\alpha_p = \alpha_m \gg \alpha_g$, and this implies that when the heat process of the glass starts, the heat processes of the plunger and the mould are already in the steady state. This means that the temperature $T_p = T_p(0)$ and $T_m = T_m(0)$. Hence the three heat processes are not coupled.

Now we have for the glass process the following boundary value problem

$\frac{1}{k_g}\frac{\partial T_g}{\partial t} = \Delta T_g$ in Ω_g.

The boundary conditions are given by $\frac{\partial T_g}{\partial n} = 0$ on $\Gamma_g \cup \Gamma_{ga}$,
$k_g \frac{\partial T_g}{\partial n} = h_{gp}(T_g - T_{0p})$ on Γ_{gp},
$k_g \frac{\partial T_g}{\partial n} = h_{gm}(T_g - T_{0m})$ on Γ_{gm},

where h_{gp} is the contact conductance between the glass and the plunger and h_{gm} is the contact conductance between the glass and the mould. The contact conductance depends on the surface roughness, the interface pressure and temperature, the thermal conductivities of the contacting materials and the type of fluids or gas in the gap, and is about $h_{gp} = h_{gm} = 2 \cdot 10^3$[W/m^2/.$c$].

On the two boundaries Ω_{gp} and Ω_{gm} we have a temperature drop, depending on the contact conductances, and a boundary layer, depending on the thermal diffusivity of the glass. One can prove that the asymptotic behaviour of the boundary layer is the errorfunction erfc$(r/\sqrt{4k_g t})$.

6 Computation of the flow

Since we now may assume the flow to be isothermal after all we can concentrate on solving the Stokes equation, subject to kinematic boundary conditions. So consider the configuration in fig.6.1 Let $\Gamma_t = \partial\Omega_t$ be the boundary of Ω_t. It is easy to

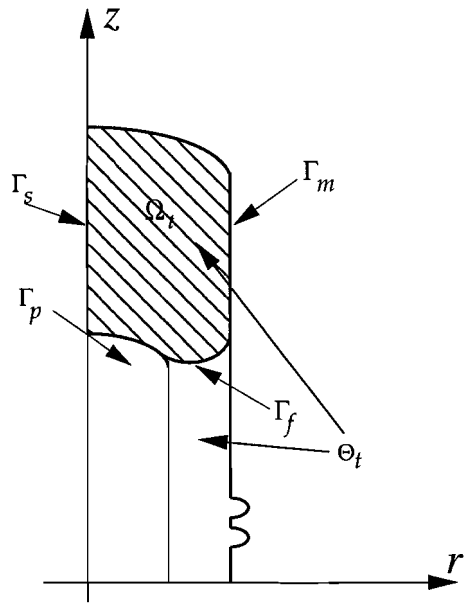

Figure 6.1: 2-D domain.

see that Γ_t consists of four parts:

$$\Gamma_t = \Gamma_m \cup \Gamma_f \cup \Gamma_p \cup \Gamma_s,$$

corresponding to the mould, free boundary, plunger, and symmetric part respectively. As glass during the process is assumed to be a fluid, no-slip boundary conditions can be assumed for correspondent parts of boundary Γ_t:

$$\begin{aligned} \mathbf{v} &= \mathbf{v}_p, \\ \mathbf{v} &= 0, \end{aligned} \tag{6.1}$$

where $\mathbf{v}_p$ is the velocity of the plunger.

A symmetry boundary condition is required for Γ_s:

$$\begin{aligned} \mathbf{v}_n &= 0, \\ \frac{\partial \mathbf{v}_s}{\partial n} &= 0, \\ \frac{\partial p}{\partial n} &= 0. \end{aligned} \tag{6.2}$$

At the free boundary the normal stress must be equal to the external pressure p_0, which is assumed to be constant. The tangential stress must be equal to zero. Hence:

$$\begin{aligned} p - 2\mu \frac{\partial \mathbf{v}_n}{\partial n} &= p_0, \\ \frac{\partial \mathbf{v}_n}{\partial t} + \frac{\partial \mathbf{v}_s}{\partial n} &= 0. \end{aligned} \tag{6.3}$$

One should note that (6.1) provides for kinematic boundary conditions. Indeed, the domain Ω_t, corresponding to the region occupied by the glass at time t, is time-dependent and changes during the process. The method of solution is now to use a Stokes solver (we actually use a finite element method) on the domain Ω_t, and employ the thus found velocity field to simulate the evolution.

Let $\mathbf{x} : [0, T] \times \Omega_0 \to \mathbb{R}^2$ be such a mapping that:

$$\mathbf{x}(0) = \Omega_0, \quad \mathbf{x}(t) = \Omega_t,$$

where Ω_t is the problem domain as defined before. Then the relation between the velocity field and the domain geometry can be described by the initial value problem:

$$\begin{aligned} \frac{d\mathbf{x}(t)}{dt} &= \mathbf{v}(\mathbf{x}(t)), \quad t \in [0, T], \\ \mathbf{x}(0) &= \Omega_0 \end{aligned} \tag{6.4}$$

The velocity field $\mathbf{v}(\mathbf{x}(t))$ can be obtained by solving Stokes equations in Ω_t. However, one should realize that the geometry of Ω_t depends on that velocity field.

In order to overcome this problem we will use the following strategy. Let us define

$$t_n = n\Delta t, \quad n = 1, \ldots, N,$$

such that $t_0 = 0$, $t_N = T$. After discretization and solving Stokes equations with correspondent boundary conditions in Ω_{t_n} (which are assumed to be defined) we obtain the velocity field $\mathbf{v}^n$. Instead of (6.4) we solve the initial value problem:

$$\begin{aligned} \frac{d\mathbf{x}(t)}{dt} &= \mathbf{v}^n, \quad t \in [t_n, t_{n+1}], \\ \mathbf{x}(t_n) &= \Omega_{t_n}. \end{aligned} \tag{6.5}$$

At a particular for any point $\mathbf{x}_i^n$ on the free boundary Γ_f we may consider this as a Lagrangian displacement, which we may e.g. discretize by the explicit Euler method:

$$\mathbf{x}_i^{n+1} = \mathbf{x}_i^n + \Delta t \mathbf{v}_i^n. \tag{6.6}$$

The local error for this algorithm is of the first order in Δt.

The geometry of $\Omega_{t_{n+1}}$ can be obtained now, and hence the boundary conditions required for solving the flow equations at t_{n+1} can be defined. The same procedure is repeated then until the final geometry Ω_{t_N} and corresponding flow quantities will have been computed. Instead of Euler explicit it is possible to use more sophisticated integration schemes. For our problem it turns out to be one of the most important aspects.

Consider first in more detail the deformation of the free boundary during a time step. Applying formula (6.6) for a point $\mathbf{x}_i^n$ at the boundary Γ_f^n (i.e. the boundary Γ_f at time t_n) with corresponding velocities $\mathbf{v}_i^n$, we see that some of the points $\mathbf{x}_i^{n+1}$ don't belong to the domain as defined by the mould and the plunger. Let us denote the latter by $\Theta_{t_{n+1}}$. This configuration is changed explicitly by moving the plunger at each time iteration. We now simply clip displacement outside this $\Theta_{t_{n+1}}$, see fig.6.2. So the position of $\mathbf{x}_i^{n+1}$ is defined now by intersection of $\mathbf{x}_i^{n+1} + span\{\mathbf{v}_i^n\}$ and $\Theta_{t_{n+1}}$

$$\mathbf{x}_i^{n+1} = \mathbf{x}_i^n + \alpha_i \Delta t \mathbf{v}_i^n, \quad \alpha_i \in (0, 1]. \tag{6.7}$$

Here α_i is chose such that

$$\Omega_{t_{n+1}} \subset \Theta_{t_{n+1}}.$$

We shall call this algorithm the *clip algorithm*. Note that for the local error in (6.7) we have

$$\frac{\|\mathbf{x}_i(t_{n+1}) - \mathbf{x}_i^{n+1}\|}{\Delta t} = \frac{\|\mathbf{x}_i(t_n) + \Delta t \dot{\mathbf{x}}_i(t_n) - \mathbf{x}_i^n - \alpha_i \Delta t \mathbf{v}_i^n\|}{\Delta t} + O(\Delta t) =$$

$$\frac{\|\mathbf{x}_i(t_n) + \Delta t \dot{\mathbf{x}}_i(t_n) - \mathbf{x}_i(t_n) - \alpha_i \Delta t \dot{\mathbf{x}}_i(t_n)\|}{\Delta t} + O(\Delta t) =$$

$$(1 - \alpha_i)\|\dot{\mathbf{x}}_i(t_n)\| + O(\Delta t).$$

For the velocities that must be clipped ($\alpha_i < 1$) the error is apparently $O(1)$, although their contribution to the global error is still $O(h)$.The actual values of α_i depend on the characteristics of the process, Δt and the mesh size h. In a practical implementation the term $(1 - \alpha_i)\|\dot{\mathbf{x}}_i(t_n)\|$ should be of order Δt.

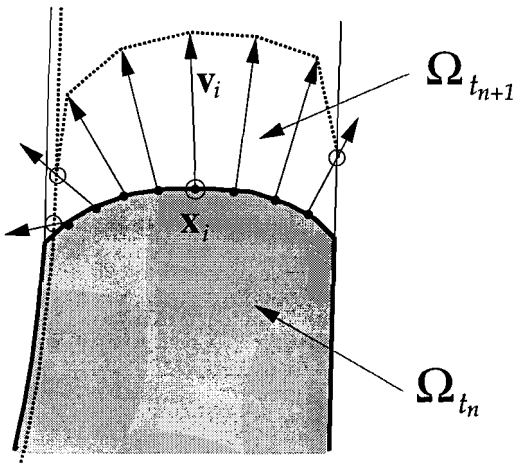

Figure 6.2: Clip algorithm.

7 Mass conservation

In the previous section we described one step of the actual solution process, i.e. solving Stokes, doing one Euler step, and clipping "non physical" values. Clearly the latter procedure leads to the question whether mass is still conserved. The finite volume of glass (which can be associated with the mass because of incompressibility) is given a priori and equal to Θ_{t_N}, i.e. the volume of mould-plunger system in its final position, when the final domain is filled with glass. Numerically we may find the mass decreasing or increasing. If this is significant (say more than 1 %) the simulation process is useless. For example, in the case of mass decreasing we can see that there is space left in Θ_{t_N} and $\Theta_{t_N} \backslash \Omega_{t_N} \neq \{\emptyset\}$.

In order to solve this problem we can perform the process with a smaller time step, which requires more computational time for solving the flow equations, or increase accuracy of numerical integration by using scheme of higher order. Increasing of mass (fig.7.1) arises because of Euler explicit, as it is not a conservative scheme. Instead of (6.3) we shall use the following trapezoidal like algorithm:

$$\begin{aligned} \mathbf{y}_i^0 &= \mathbf{x}_i^0, \\ \mathbf{y}_i^{n+1} &= \mathbf{x}_i^n + \Delta t \mathbf{v}_i^n, \\ \mathbf{x}_i^{n+1} &= \mathbf{x}_i^n + \frac{\Delta t}{2}(\mathbf{v}_i^n + \mathbf{v}_i^{n+1}), \end{aligned} \tag{7.1}$$

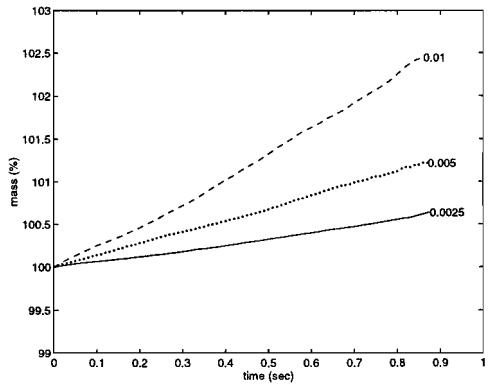

Figure 7.1: Volume graph using Euler explicit and different time steps.

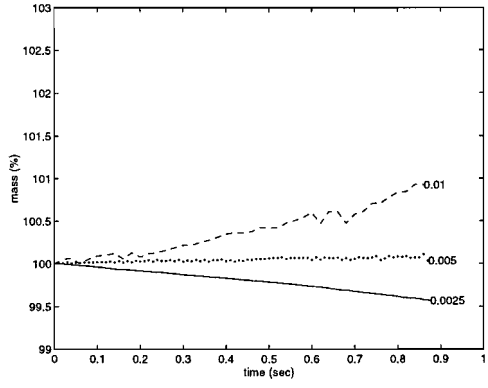

Figure 7.2: Volume graph for second order scheme and different time steps.

where $\mathbf{v}_i^n$ now is the velocity at $\mathbf{y}_i^n$. The advantage of this explicit predictor-corrector scheme is that the velocity field has to be calculated only once each time step. It is still not conservative but at least of higher order. With respect to mass conservation, simulation using the combination of the clip algorithm and (6.6) is illustrated by fig.7.2. The mass still increases for $\Delta t = 0.01$ because the scheme is still explicit. The local error in (6.6) is of second order with respect to Δt, the discretization error in clip algorithm is of lower order; hence, for a smaller time step ($\Delta t = 0.0025$) we can see that the clip algorithm, which decreases mass by clipping the velocities, dominates. The graph for $\Delta t = 0.005$, which gives almost mass conservation, is a case where Euler explicit and clip algorithms errors cancel more or less.

Using a FEM method to solve the Stokes equations and (7.1) to obtain the changing geometry of Ω_t we can run numerical simulations up to the final stage. The

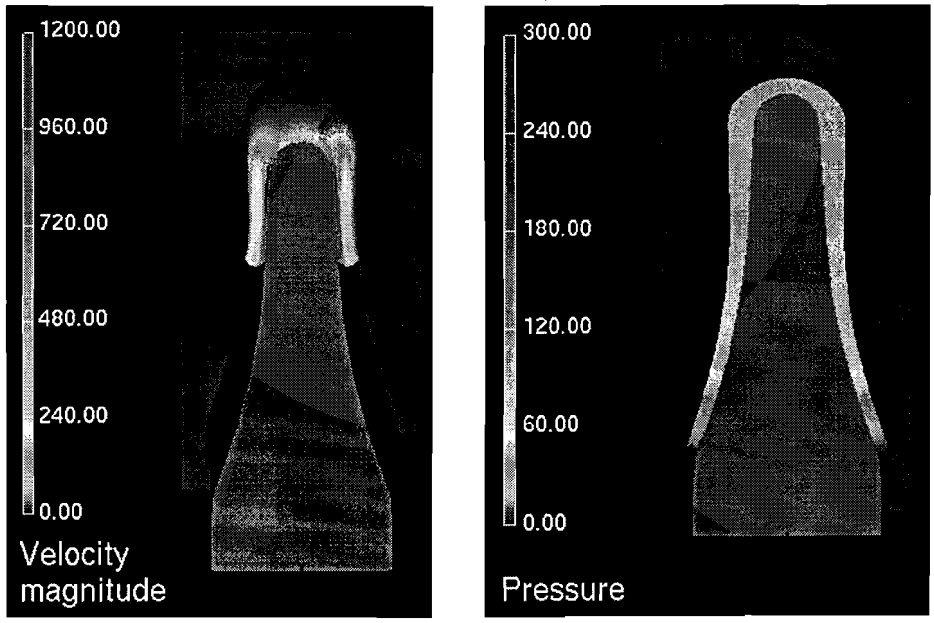

Figure 7.3: Velocity magnitude and pressure.

final results are depicted in fig.7.3.

References

[1] T.D. Chandra, S.W. Rienstra, *Analytical Approximation to the Viscous Glass Flow Problem in the Mould-Plunger Pressing Process*, RANA 97-08, Technical University of Eindhoven,1997.

[2] P.J. Doyle, *Glass Making Today*, R.A.N. Publisher, Ohio, 1994.

[3] R.W. Hopper, *Plane Stokes Flow Driven by Capillarity on a Free Surface*, J. Fluid Mech. 213, 349-375, (1990).

[4] R.W. Hopper, *Plane Stokes Flow Driven by Capillarity on a Free Surface, 2: Further Developments*, J. Fluid Mech. 230, 355-364, (1991).

[5] G.C. Hsiao, P. Kopp, W.L. Wendland, *Some Applications of a Galerkin-collocation Method for Boundary Integral Equations of the First Kind*, Math. Methods in the Appl. Sciences 6, 280-325, (1984).

[6] H.K. Kuiken, R.M.M. Mattheij, G.A.L. van de Vorst, *A Boundary Element Solution for 2-dimensional Viscous sintering*, J. Comput. Phys. 100, (1992), 50-63.

[7] O.A. Ladyzhenskaya, *The Mathematical Theory of Viscous Incompressible Flow*, Godon and Beach, New York, (1963).

[8] R.M.M. Mattheij, G.A.L. van de Vorst, *Mathematical Modelling and Numerical Simulation of Viscous Sintering Processes*, Surv. Math. Ind. 7 (1998), 255-281.

[9] C.A.M. Mulder, J.G. van Lierop, G. Frens, *Densification of SiO_2-Xerogels to Glass by Ostwald ripening*, J. Noncryst. Solids 82 (1986), 92-96.

[10] H. Rawson, *Properties and Applications of Glass*, Glass Science and Technology vol.3, Elsevier, 1980.

[11] J.S. Reed, *Introduction to the Principles of Ceramic Processing*, Wiley-Interscience, Chichester, 1988.

[12] S. Sōmiya, Y. Moriyoshi (eds.), *Sintering Key Papers*, Elsevier Applied Science, London, (1990).

[13] Y.M. Stokes, *Very Viscous Flows Driven by Gravity, with Particular Application to Slumping of Molten Glass*,PhD Thesis, Univ. Adelaide, 1998.

[14] D.R. Uhlmann, V.J. Kreidl (eds), *Glass Science and Technology*, Ac. Press, London 1986

[15] G.A.L. van de Vorst, *Integral Method for a Two-Dimensional Stokes flow with Shrinking Holes, Applied to Viscous Sintering*, J. Fluid Mech. 257 (1993), 667-689.

[16] G.A.L. van de Vorst, *Modelling and Numerical Simulation of Axisymmetric Viscous Sitering*, Ph D thesis, Eindhoven, 1994.